Band structure of UPd$_3$ studied by ultrahigh-resolution angle-resolved photoemission spectroscopy

T. Ito, H. Kumigashira, S. Souma, and T. Takahashi

Department of Physics, Tohoku University, Sendai 980-8578, Japan

Y. Haga

Advanced Science Research Center, Japan Atomic Energy Research Institute, Tokai 319-1195, Japan

Y. Tokiwa and Y. Ōnuki

Advanced Science Research Center, Japan Atomic Energy Research Institute, Tokai 319-1195, Japan and Department of Physics, Osaka University, Toyonaka 560-0043, Japan

We have performed ultrahigh-resolution angle-resolved photoemission spectroscopy on UPd$_3$ to study the band structure near the Fermi level (E_F) and the Fermi surface. We found three Fermi surfaces (FS's): two hole pockets with a dominant Pd $4d$ character at the Γ (A) point and an electron pocket with a U $6d$ nature at the K (H) point. These FS's are qualitatively well reproduced in the band structure calculation based on the localized U-$5f$-electron model, while remarkable quantitative discrepancies are observed near E_F. The U $5f$ states are located 0.4–1.0 eV below E_F and do not contribute to the Fermi surface. These results indicate the strongly localized nature of U $5f$ electrons in UPd$_3$.

I. INTRODUCTION

UPd$_3$ has been regarded as an exceptional U-based intermetallic compound possessing "localized" U $5f$ electrons[1–10] in contrast to many other U-based intermetallic compounds such as UPt$_3$ and URu$_2$Si$_2$, where U $5f$ electrons form very narrow band(s) at or near the Fermi level (E_F) and behave as very heavy "itinerant" electrons.[11–13] It is recognized that the large variety of physical properties of U compounds stems from the intrinsic nature of U $5f$ electrons with a duality of "itinerant" and "localized" natures. The observed anomalous properties of UPd$_3$ have been attributed to the "localized" U $5f$ electrons.[1–10] UPd$_3$ exhibits a three-staged magnetic phase transition as a function of temperature from the paramagnetic phase to the first quadrupolar phase at $T_Q = 7.5$ K, then to the second quadrupolar phase at $T'_Q = 6.5$ K, and finally to the antiferromagnetic phase at 4.5 K (Refs. 2 and 9). Early angle-integrated photoemission studies[14–18] have shown that the U $5f$ states are situated about 1 eV below E_F in contrast to "itinerant" U compounds where the U $5f$ "bands" are located at E_F.[19–24] The crystal-field splitting of U^{4+} ions was observed by inelastic neutron scattering.[1–4] Further, the effective mass of carriers estimated from de Haas–van Alphen (dHvA) experiments[8–10] and the electronic specific heat coefficient[6–8] is very small compared with that of U-based heavy-fermion materials. All these experimental results strongly suggest that U $5f$ electrons in UPd$_3$ are "localized" and form flat "band(s)" far away from E_F. However, there are some reports against this picture. The Fermi surface (FS) topology obtained from the dHvA measurements[8,9] is not consistent with the band structure calculation which treats the U $5f$ electrons as "localized" states.[25] Furthermore, the experimentally obtained magnetic moment in the antiferromagnetic state ($\sim 10^{-2} \mu_B$) (Refs. 1

and 2) is considerably smaller than that of a U^{4+} ion ($3.58\mu_B$) expected from the localized model.[26] Such a small magnetic moment is rather a common feature in U-based heavy-fermion superconductors[13,27,28] and is regarded as a evidence for the intermediate valence of U ions.[29] Thus the "localized" nature of U $5f$ electrons in UPd$_3$ is now questioned and a new experimental input from a different viewpoint is necessary to resolve the present controversy.

In this paper, we report high-resolution angle-resolved photoemission spectroscopy (ARPES) on UPd$_3$ to study the "band structure" near E_F as well as the Fermi surface. By using high-energy (15 meV) and angular ($\pm 0.1°$) resolutions, we have succeeded in mapping out the detailed "band structure" near E_F and the Fermi surface. We compare the present ARPES results with the band structure calculation[25] as well as the dHvA experiments[8–10] and thereby discuss the nature of U $5f$ electrons in UPd$_3$.

II. EXPERIMENT

UPd$_3$ single crystals (typically 3–4 mm in diameter and 75 mm in length) were grown by the Czochralski method with a tetra-arc furnace. Starting materials were 99.95% pure U and 99.999% pure Pd in the respective molar ratios. The x-ray diffraction, electrical resistivity, magnetic susceptibility, and specific heat measurements have been performed for characterization, and the results show good agreement with those reported earlier.[8,9] ARPES measurements were performed using a SCIENTA SES-200 spectrometer with a high-flux discharge lamp and a toroidal grating monochromator. We used the He $I\alpha$ resonance line (21.218 eV) to excite photoelectrons. The energy resolution was set at 15 meV for quick data acquisition because of the relatively fast degradation of the crystal surface. The angular resolution was $\pm 0.1°$, which corresponds to a momentum resolution
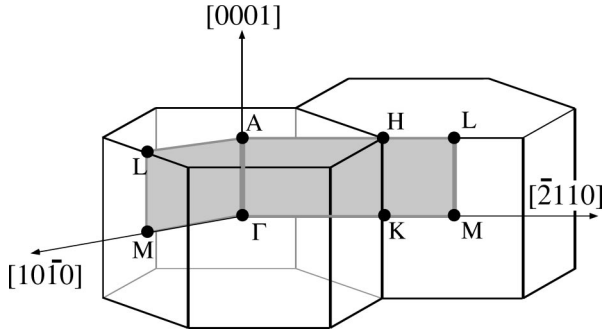
FIG. 1. Brillouin zone of paramagnetic UPd_3 in the extended zone scheme. Shaded areas correspond to measured ΓKM-LHA and ΓM-LA planes.

comparable to 1% of the whole Brillouin-zone length. Single crystals were cleaved *in situ* at 25 K just before measurement under an ultrahigh vacuum of 4×10^{-11} Torr. ARPES measurements were performed for the clean mirrorlike surface along ΓKM-LHA and ΓM-LA emission planes in the double hexagonal Brillouin zone of UPd_3 (see Fig. 1). The Fermi level of samples was referenced to that of a gold film evaporated on the sample substrate. We have confirmed the reproducibility of data on several different surfaces and samples.

III. RESULTS AND DISCUSSION

Figures 2 and 3 show ARPES and momentum distribution curve (MDC) spectra along ΓKM and ΓM high-symmetry lines in the double hexagonal Brillouin zone (Fig. 1), respectively. These two different types of spectra represent essentially the same electronic structure; the ARPES spectrum is an energy distribution curve (EDC) defined as the photoemission intensity as a function of binding energy at a fixed wave vector while the MDC spectrum is defined as the photoemission intensity as a function of wave vector at a fixed binding energy. Although EDC spectra have been routinely used to study the band structure of materials so far, MDC spectra have some principle advantages over EDC, in particular, in analysis of the electronic structure near E_F (Ref. 30). For example, (1) the background effect from the secondary electrons is easily removed in the MDC spectrum while the EDC spectrum has a large binding-energy-dependent background due to the secondary electrons, and (2) the MDC spectrum does not suffer the Fermi-edge-cutoff effect since the Fermi-Dirac function has the same value at a fixed binding energy. It is naturally expected that the MDC spectrum is sensitive to steeply dispersive bands while EDC to slowly dispersive bands. In fact, several highly dispersive bands symmetric with respect to the Γ (A) or M (L) point are clearly seen in the MDC spectra in Fig. 3, while almost flat bands appear in the EDC (ARPES) spectra in Fig. 2. It is remarked that there is no sharp peak at E_F in the EDC spectra (Fig. 2), which has been commonly observed in U-based heavy-fermion materials and is ascribed to the Kondo-resonance peak.[22,23] This suggests the localized nature of U $5f$ electrons in UPd_3.

In order to study the electronic structure near E_F as well as the nature of U $5f$ electrons in UPd_3 in detail, we display
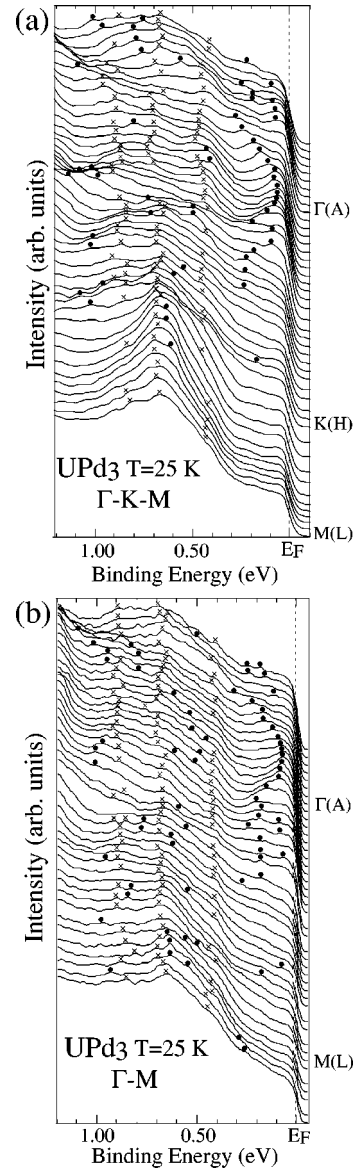

FIG. 2. High-resolution ARPES spectra near E_F of UPd_3 along (a) ΓKM (AHL) and (b) ΓM (AL) high-symmetry lines measured with He $I\alpha$ photons at 25 K. Solid circles and crosses indicate peak positions of dispersive and nondispersive features, respectively.

in Fig. 4 the experimentally derived band structure along the ΓKM and ΓM directions, compared with the band structure calculation based on the localized U-$5f$-electron model.[25] The experimental band dispersions were obtained by plotting the peak position as a function of the wave vector and the binding energy for both EDC and MDC spectra.[31] The experimental bands in Figs. 4(a) and 4(b) are categorized roughly into two groups: (1) highly dispersive bands extending all over the Brillouin zone and (2) three nondispersive bands located at 0.4–1.0 eV. According to photon-energy-dependent angle-integrated PES studies,[14–18] the highly dispersive bands are attributed to Pd $4d$ and U $6d$ electrons while the flat bands have a strong U $5f$ character. We find in Figs. 4(a) and 4(b) that the experimental bands show symmetric dispersion with respect to the K (H) or M (L) point
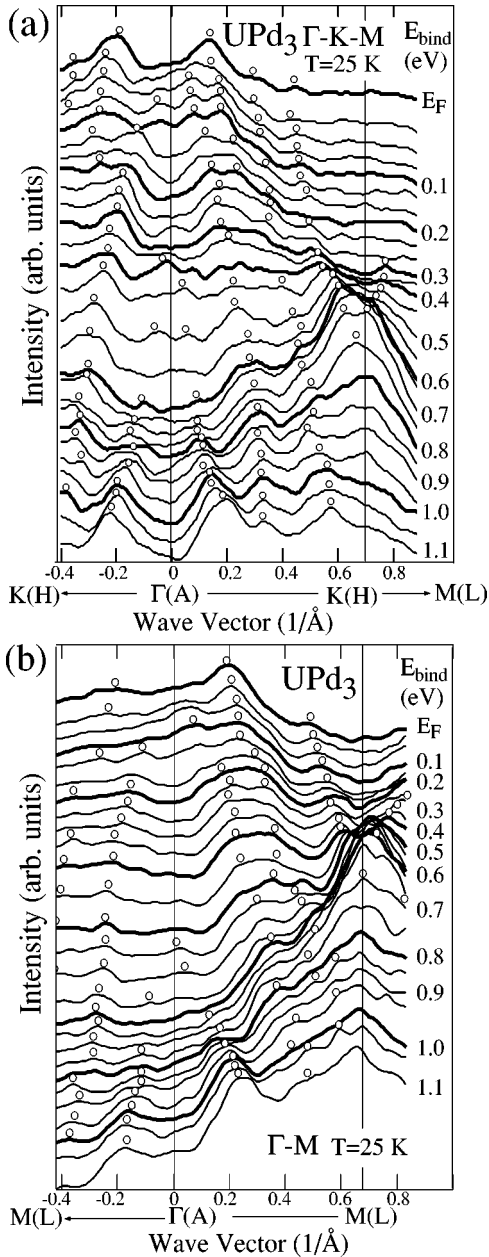
FIG. 3. MDC spectra near E_F of UPd$_3$ along (a) ΓKM (AHL) and (b) ΓM (AL) high-symmetry lines. Open circles indicate peak positions of dispersive features.

and the dispersions have the periodicity matching very well with the bulk Brillouin zone. This indicates that the observed bands are of bulk origin.[32,33] Furthermore, the band dispersion shows a qualitatively good agreement with the band structure calculation where the U $5f$ electrons are treated as localized states.[25] All these results strongly suggest that the U $5f$ electrons are substantially localized, forming nondispersive bands away from E_F, while the Pd $4d$–U $6d$ hybridized states form highly dispersive bands and give the Fermi surface in UPd$_3$.

In the localized picture, the U-$5f$-originated peaks in PES spectra have been interpreted in terms of the U-$5f^1$-final-state (U^{4+}) multiplet[14,15] which consists of two

spin-orbit components ($^2F_{5/2}$ and $^2F_{3/2}$) with an energy separation of 0.9 eV (Refs. 34 and 35). In contrast, we find "three" U $5f$ "bands" in Figs. 4(a) and 4(b). Furthermore, the energy separation between each U $5f$ "band" is slightly different from the theoretical value for the multiplet structure. One probable explanation for this discrepancy is that these three U $5f$ "bands" consist of two different multiplet structures. Since there are two different U sites in the paramagnetic UPd$_3$ with a double hexagonal crystal structure,[8,36] the Madelung energy and consequently the U $5f$ bare level are expected to be different between the cubic and the hexagonal sites. In fact, two different magnetic excitations ascribable to the two sites have been observed in the inelastic neutron scattering.[1-4]

Next, we discuss the band structure near E_F of UPd$_3$, which is found to consist of mainly Pd $4d$–U $6d$ hybridized states according to the discussion above. We find at first that the overall band dispersion agrees well between the experiment and calculation. For example, the experimental bands c (c') and d (d'), which form hole pockets at the Γ (A) point, correspond to the calculated bands T^2 (Σ^2) and T^3 (Σ^3) with a dominant Pd $4d$ character. In addition, the experimental band e at the K (H) point corresponds to a group of three theoretical bands (T^4, S^4, and S^5) with a strong U $6d$ character. This good agreement between the experiment and calculation suggests that the localized U-$5f$-electron model is a good starting point in understanding the electronic structure of UPd$_3$. On the other hand, we find several quantitative discrepancies in the close vicinity of E_F. The bottom of experimental band e with a dominant U $6d$ character is located at 650 meV from E_F at the K (H) point, while that of corresponding bands in the calculation (T^4, S^4, and S^5) is around 150 meV. Furthermore, we find that two parabolic bands a (a') and b (b') at the Γ (A) point with a Pd $4d$ character have the top at 400 and 50 meV below E_F, respectively, and are totally occupied, while the calculation predicts the E_F crossing of the corresponding bands [T^1, S^2, and S^3 (Σ^2, R^2, and R^3)]. This discrepancy in the relative energy position of the Pd $4d$ and U $6d$ bands between the experiment and calculation may be attributed to underestimation of the Pd $4d$–U $6d$ hybridization strength in the calculation. Since the dHvA results have been analyzed based on this band calculation,[8,10] the discrepancy observed by the present ARPES study strongly requests a reinterpretation of the FS topology of UPd$_3$.

In order to study the FS topology of UPd$_3$ in detail, we show MDC curves at E_F along the two high-symmetry lines in Fig. 5, together with the experimental band dispersions in the close vicinity of E_F. In the ΓKM (AHL) direction, we find peaks at ± 0.18 Å^{-1} in the MDC spectrum which correspond to the k_F of band c, followed by two small peaks at 0.33 Å^{-1} and 0.48 Å^{-1} which correspond to the k_F's of bands d and e, respectively. In the ΓM (AL) direction, on the other hand, we find a large peak at 0.18 Å^{-1} and a small one at 0.46 Å^{-1}, which correspond to the k_F's of bands c' and d', respectively. By taking account of the sixfold symmetry of the Brillouin zone, we have roughly mapped out the Fermi surface of UPd$_3$ projected onto the (0001) plane as shown in
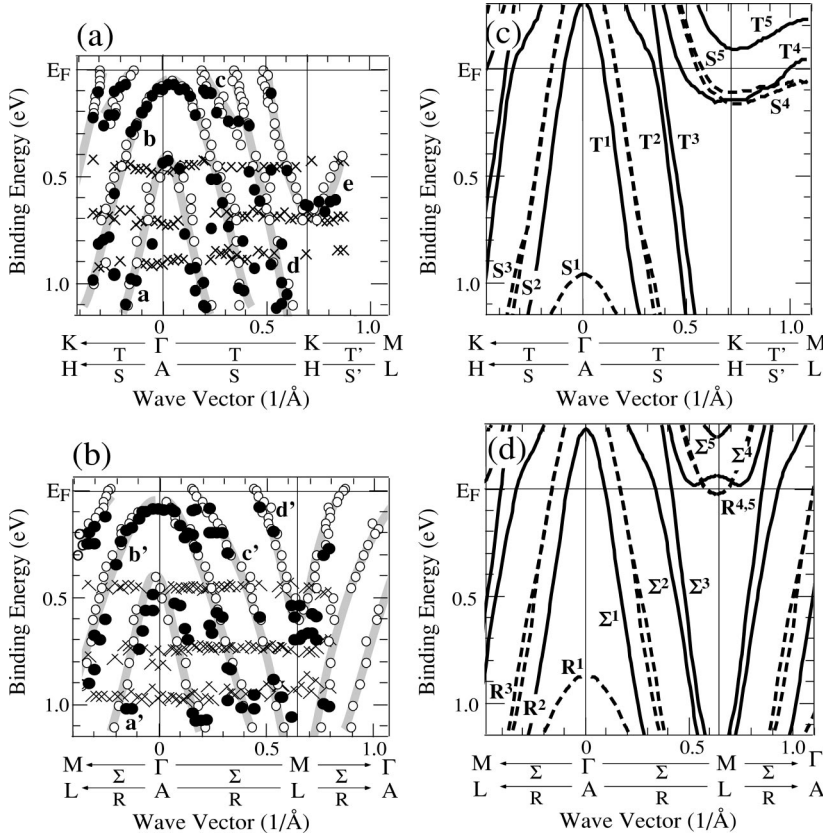
FIG. 4. Experimental band structures near E_F of UPd$_3$ along (a) ΓKM (AHL) and (b) ΓM (AL) high-symmetry lines. Open and solid circles and crosses correspond to the peak positions in EDC and MDC spectra (Figs. 2 and 3). Note that the same symbols are used in Figs. 2–4. Gray thick lines are a guide for the eye. The band structure calculation based on the localized U-5f-electron model (Ref. 25) along (c) ΓKM (AHL) and (d) ΓM (AL) high-symmetry lines is shown for comparison.

Fig. 6, where solid circles, triangles, and squares correspond to the Fermi momenta k_F^c ($k_F^{c'}$), k_F^d ($k_F^{d'}$), and k_F^e, respectively. As described above, the Fermi momenta k_F^c ($k_F^{c'}$) and k_F^d ($k_F^{d'}$) correspond to the holelike FS's at the Γ (A) point formed by the Pd 4d bands c (c') and d (d'), while the momentum k_F^e corresponds to an electronlike FS at the K (H) point formed by the U 6d band e.

Table I summarizes physical parameters (k_F, character, size, and effective mass) of the Fermi surfaces in UPd$_3$ ob-

tained by the present ARPES, compared with those from the dHvA experiments[8,9] and the band calculation.[25] In estimating the size, we assumed a circular or star-shaped Fermi surface as shown in Fig. 6. We call these two holelike and one electronlike experimental FS's as Fermi surfaces C, D, and E, respectively. The dHvA experiments have reported several independent FS's (α, β, γ, δ, ζ, and ϵ).[8,9] Since the FS's α and ζ are assigned to the open orbits, we excluded these two FS's from the comparison and assumed a circular shape for the other FS's in estimating the k_F and size. We
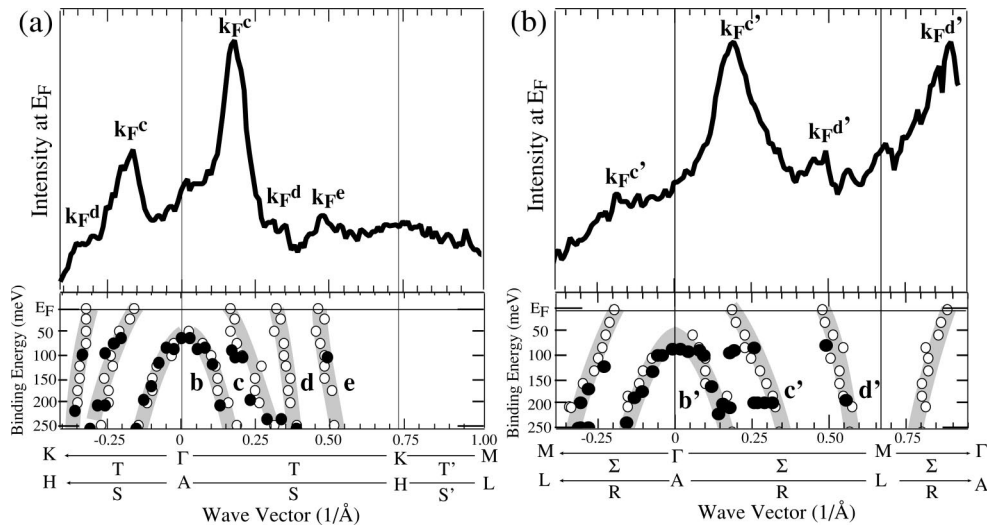

FIG. 5. MDC spectra at E_F (energy window is ± 7.5 meV) of UPd$_3$ for (a) ΓKM (AHL) and (b) ΓM (AL) high-symmetry lines. To highlight the steep dispersive features, the experimental band dispersion near E_F is shown in lower panel.
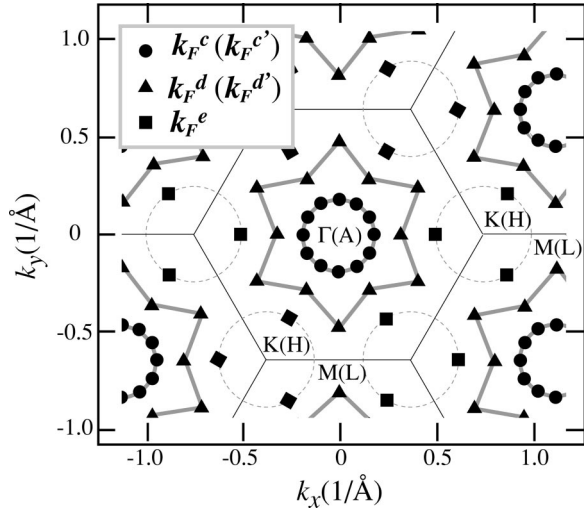
FIG. 6. Fermi surfaces of UPd$_3$ projected onto the (0001) plane, determined by the present ARPES experiment. Solid circles, triangles, and squares correspond to the k_F^c ($k_F^{c'}$), k_F^d ($k_F^{d'}$), and k_F^e in Fig. 5, respectively. Gray solid and dashed lines are a guide for the eye.

find in Table I that the Fermi surfaces C and D in the ARPES experiment correspond to the δ and β orbits in the dHvA experiment. The electronlike FS at the K (H) point (Fermi surface E in ARPES) probably corresponds to the orbit γ in dHvA experiment. In spite of this qualitative good agreement between the ARPES and dHvA experiments, it is again noted here that the assignment of FS's in the dHvA experiment were based on the band calculation shown in Fig. 4 which apparently contradicts the ARPES result. The calculated band T^1 (Σ^1), which was assigned to the orbit δ in the dHvA study, is found to be totally occupied and not to contribute to the Fermi surface as shown in Fig. 4. Therefore, the assignment of each orbit observed in the dHvA experiment should be corrected as in Table I.

Finally, we briefly comment on the effective mass in UPd$_3$ in comparison with the dHvA measurements[8–10] as well as the thermodynamic properties.[6–8] From the band dispersions obtained by ARPES, we have estimated the effective mass for each dispersion with the free-electron approximation and compared them with the cyclotron effective masses obtained from the dHvA experiment[8,10] in Table I. We find that the effective masses obtained from the ARPES and dHvA experiments agree with each other almost perfectly and both show very small effective masses ($\sim 2m_0$) compared with those in heavy-fermion U compounds [$\sim 10^2 m_0$ (Refs. 11–13)]. The observed small mass enhancement is consistent with the small electronic specific heat coefficient[6,7] of UPd$_3$ ($\gamma \sim 9.5$ mJ/mol K^2) compared with those of heavy-fermion compounds [>400 mJ/mol K^2 (Ref. 11)].

IV. CONCLUSION

We have studied the electronic band structure near E_F and the Fermi surface of UPd$_3$ using ultrahigh-resolution angle-resolved photoemission spectroscopy. We have observed several highly dispersive bands forming the Fermi surfaces as well as nondispersive "bands" near E_F, which are ascribed to the Pd $4d$–U $6d$ hybridized bands and the U $5f$ states, respectively. The overall band structure consisting of the Pd $4d$–U $6d$ hybridized states shows a qualitative good agreement with the band calculation based on the localized U-$5f$-electron model,[25] indicating that the band structure calculation serves as a good starting point in understanding the gross electronic structure of UPd$_3$ and at the same time the U $5f$ electrons are strongly localized in UPd$_3$. We have observed three Fermi surfaces: two holelike FS's with a dominant Pd $4d$ character at the Γ (A) point and an electronlike FS with a U $6d$ nature at the K (H) point. The size and effective mass of the observed FS's are consistent with the dHvA measurements[8,10] and the thermodynamic properties,[6–8] while the previous assignment of FS's in the dHvA experiment should be corrected because of the possible underestimation of the Pd $4d$–U $6d$ hybridized strength in the band calculation. The present ARPES results suggest that the localized character of U $5f$ electrons plays an essential role in characterizing the magnetic properties of UPd$_3$.

TABLE I. Fermi momentum (k_F), character, size, and effective mass of the Fermi surfaces of UPd$_3$ obtained by the present ARPES experiment and the dHvA experiments (Refs. 8–10). Note that the previous assignment of FS's in the dHvA experiment should be corrected because of the possible underestimation of the Pd $4d$–U $6d$ hybridized strength in the band calculation (Ref. 25).

		k_F (Å^{-1})	Character	Size (Å^{-2})	Effective mass (m_0)	Assignment	
ARPES	c (c')	0.18 (0.18)	Hole	0.10	2.6 (2.6)	T^2 (Σ^2)	
	d (d')	0.33 (0.46)	Hole	0.46	1.6 (2.6)	T^3 (Σ^3)	
		[from Γ (A)]					
	e	0.24	Electron	≥ 0.18	1.6	T^4, S^4, S^5	
		[from K (H)]					
						Previous	Corrected
dHvA	β	0.39	Hole	0.48	1.79–2.69	S^2 (R^2)	T^3 (Σ^3)
	γ	0.28		0.24	2.49–2.60		T^4, S^4, S^5
	δ	0.20	Hole	0.12	~ 1.66	T^1 (Σ^1)	T^2 (Σ^2)
	ϵ	0.10	Electron	0.03	0.45–0.69	S^5 (R^5)	

[1] M.J. Bull, K.A. McEwen, R. Osborn, and R.S. Eccleston, Physica B **223&224**, 175 (1996).

[2] K.A. McEwen, U. Steigenberger, K.N. Clausen, Y.J. Bi, M.B. Walker, and C. Kappler, Physica B **213&214**, 128 (1995); K.A. McEwen, U. Steigenberger, and J.L. Martinez, *ibid.* **186-188**, 670 (1993).

[3] N. Shamir, M. Melamud, H. Shaked, and M. Weger, Physica B **94**, 225 (1978).

[4] W. J. L. Buyers and T. M. Holden, in *Handbook on the Physics and Chemistry of the Actinides*, edited by A. J. Freeman and G. H. Lander (Elsevier Science, Amsterdam, 1985), Vol. 2, p. 239.

[5] J. Schoenes and K. Andres, Solid State Commun. **42**, 359 (1982).

[6] K. Andres, D. Davidov, P. Dernier, F. Hsu, W.A. Reed, and G.J. Nieuwenhuys, Solid State Commun. **28**, 405 (1978).

[7] Y. Ōnuki, T. Yamazaki, I. Ukon, T. Komatsubara, A. Umezawa, W.K. Kwok, G.W. Crabtree, and D.G. Hinks, J. Phys. Soc. Jpn. **58**, 2119 (1989).

[8] S.W. Yun, H. Sugawara, J. Itoh, M. Takashita, T. Ebihara, N. Kimura, P. Svoboda, R. Settai, Y. Ōnuki, and H. Sato, J. Phys. Soc. Jpn. **63**, 1518 (1994).

[9] Y. Tokiwa, K. Sugiyama, T. Takeuchi, R. Settai, Y. Inada, Y. Haga, E. Yamamoto, T. Honma, K. Sakurai, M. Nakashima, K. Miyake, K. Kindo, and Y. Ōnuki, Physica B **281&282**, 604 (2000).

[10] W. Ubachs, A.P.J. van Deursen, A.R. de Vroomen, and A.J. Arko, Solid State Commun. **60**, 7 (1986).

[11] R.H. Heffner and M.R. Norman, Comments Condens. Matter Phys. **17**, 361 (1996); G.R. Stewart, Rev. Mod. Phys. **56**, 755 (1984).

[12] For example, G. Zwicknagl, Adv. Phys. **41**, 203 (1992); M.B. Maple, M.C. de Andrade, J. Herrmann, Y. Dalichaouch, D.A. Gajewski, C.L. Seaman, R. Chau, R. Movshovich, M.C. Aronson, and R. Osborn, J. Low Temp. Phys. **99**, 223 (1995); F. Steglich, C. Geibel, R. Modler, M. Lang, P. Hellmann, and P. Gegernwart, *ibid.* **99**, 267 (1995).

[13] H. R. Ott and Z. Fisk, in *Handbook on the Physics and Chemistry of the Actinides*, edited by A. J. Freeman and G. H. Lander (Elsevier Science, Amsterdam, 1987), Vol. 2, p. 85.

[14] B. Reihl, N. Mårtensson, D.E. Eastman, A.J. Arko, and O. Vogt, Phys. Rev. B **26**, 1842 (1982).

[15] Y. Baer, H.R. Ott, and K. Andres, Solid State Commun. **36**, 387 (1980).

[16] J.-S. Kang, J.W. Allen, M.B. Maple, M.S. Torikachvili, W.P. Ellis, B.B. Pate, Z.-X. Shen, J.J. Yeh, and I. Lindau, Phys. Rev. B **39**, R13 529 (1989).

[17] L.Z. Liu, J.W. Allen, C.L. Seaman, M.B. Maple, Y. Dalichaouch, J.-S. Kang, M.S. Torikachvili, and M.A. Lopez de la Torre, Phys. Rev. Lett. **68**, 1034 (1992).

[18] J.D. Denlinger, J.W. Allen, S.-H. Yang, S.-J. Oh, E.-J. Cho, W.P. Ellis, D.A. Gajewski, R. Chau, and M.B. Maple, Physica B **259-261**, 1130 (1999).

[19] D.D. Sarma, F.U. Hillebrecht, C. Carbone, and A. Zangwill, Phys. Rev. B **36**, 2916 (1987).

[20] B. Reihl, G. Hollinger, and F.J. Himpsel, Phys. Rev. B **28**, 1490 (1983).

[21] T. Ejima, K. Murata, S. Suzuki, T. Takahashi, S. Sato, T. Kasuya, Y. Ōnuki, H. Yamagami, A. Hasegawa, and T. Ishii, Physica B **186-188**, 77 (1993).

[22] A. J. Arko, P. S. Riseborough, A. B. Andrews, J. J. Joyce, A. N. Tahvildar-Zadeh, and M. Jarrell, in *Handbook on the Physics and Chemistry of Rare Earths*, edited by K. A. Gschneidner, Jr. and L. Eyring (Elsevier Science, Amsterdam, 1999), Vol. 26, p. 265.

[23] T. Ito, H. Kumigashira, Hyeong-Do Kim, T. Takahashi, N. Kimura, Y. Haga, E. Yamamoto, Y. Ōnuki, and H. Harima, Phys. Rev. B **59**, 8923 (1999).

[24] J.W. Allen, S.-J. Oh, L.E. Cox, W.P. Ellis, M.S. Wire, Z. Fisk, J.L. Smith, B.B. Pate, I. Lindau, and A.J. Arko, Phys. Rev. Lett. **54**, 2635 (1985).

[25] M.R. Norman, T. Oguchi, and A.J. Freeman, J. Magn. Magn. Mater. **69**, 27 (1987).

[26] J.-M. Fournier and R. Troć, in *Handbook on the Physics and Chemistry of the Actinides*, edited by A. J. Freeman and G. H. Lander (Elsevier Science, Amsterdam, 1985), Vol. 2, p. 29.

[27] G. Aeppli, E. Bucher, C. Broholm, J.K. Kjems, J. Baumann, and J. Hufnagl, Phys. Rev. Lett. **60**, 615 (1988).

[28] C. Broholm, H. Lin, P.T. Matthews, T.E. Mason, W.J.L. Buyers, M.F. Collins, A.A. Menovsky, J.A. Mydosh, and J.K. Kjems, Phys. Rev. B **43**, 12 809 (1991).

[29] V. Barzykin and Lev P. Gor'kov, Phys. Rev. Lett. **74**, 4301 (1995).

[30] T. Valla, A.V. Fedorov, P.D. Johnson, B.O. Wells, S.L. Hulbert, Q. Li, G.D. Gu, and N. Koshizuka, Science **285**, 2110 (1999).

[31] F.J. Himpsel, Adv. Phys. **32**, 1 (1983).

[32] H. Kumigashira, T. Ito, A. Ashihara, Hyeong-Do Kim, H. Aoki, T. Suzuki, H. Yamagami, T. Takahashi, and A. Ochiai, Phys. Rev. B **61**, 15 707 (2000).

[33] T. Grandke, L. Ley, and M. Cardona, Phys. Rev. B **18**, 3847 (1978).

[34] N. Beatham, P.A. Cox, A.F. Orchard, and I.P. Grant, Chem. Phys. Lett. **63**, 69 (1979).

[35] V. Kaufman and L.J. Radziemski, Jr., J. Opt. Soc. Am. A **66**, 599 (1976).

[36] A. F. Murray and W. J. L. Buyers, in *Crystalline Electric Fields and Structure Effects in f-Electrons Systems*, edited by J. E. Crow, R. P. Guertin, and T. W. Mihalisin (Plenum Press, New York, 1980), p. 257.